ACS APPLIED MATERIALS & INTERFACES

Research Article

www.acsami.org

# Tumor-Homing Cell-Penetrating Peptide Linked to Colloidal Mesoporous Silica Encapsulated (-)-Epigallocatechin-3-gallate as Drug Delivery System for Breast Cancer Therapy *in Vivo*

Jie Ding,[†,∥] Jing Yao,[‡] Jingjing Xue,[∥] Rong Li,[§] Bo Bao,[#] Liping Jiang,[∥] Jun-jie Zhu,[*,∥] and Zhiwei He[*,†]

[†]China-America Cancer Research Institute, Guangdong Medical University, Dongguan, Guangdong 523808, China

[∥]State Key Laboratory of Analytical Chemistry for Life Science, Collaborative Innovation of Chemistry for Life Science, School of Chemistry and Chemical Engineering, Nanjing University, Nanjing 210093, China

[‡]Department of Pathology, Ganzhou Health School, Ganzhou, Jiangxi 341000, China

[§]Institute of Basic Medical Sciences, Guangdong Medical University, Zhanjiang, Guangdong 524023, China

[#]Experimental Animal Center, Guangdong Medical University, Zhanjiang, Guangdong 524023, China

Supporting Information

**ABSTRACT:** Chemotherapy is the use of chemical drugs to prevent cancer cell proliferation, invasion, and metastasis, but a serious obstacle is that chemotherapeutics strikes not only on cancerous cells, but also on normal cells. Thus, anticancer drugs without side effects should be developed and extracted. (-)-Epigallocatechin-3-gallate (EGCG), a major ingredient of green tea, possesses excellent medicinal values, such as anticancer effects, DNA-protective effects, etc. However, EGCG will be mostly metabolized if it is directly orally ingested. Here, we report a drug delivery system (DDS) for loading EGCG to enhance its stability, promising target and anticancer effects *in vitro* and *in vivo*. The designed DDS is composed of three main moieties: anticancer drug, EGCG; drug vector, colloidal mesoporous silica (CMS); target ligand, breast tumor-homing cell-penetrating peptide (PEGA-pVEC peptide). Based on the results of CCK-8 assay, confocal imaging, cell cycle analysis, and Western blot, the anticancer effect of EGCG was increased by loading of EGCG into CMS and CMS@peptide. *In vivo* treatment displayed that CMS had a not obvious influence on breast tumor bearing mice, but CMS@peptide@EGCG showed the greatest tumor inhibition rate, with about 89.66%. H&E staining of organs showed no tissue injury in all experimental groups. All the above results prove that EGCG is an excellent anticancer drug without side effects and CMS@peptide could greatly promote the efficacy of EGCG on breast tumors by targeted accumulation and release, which provide much evidence for the CMS@peptide as a promising and targeting vector for DDS.

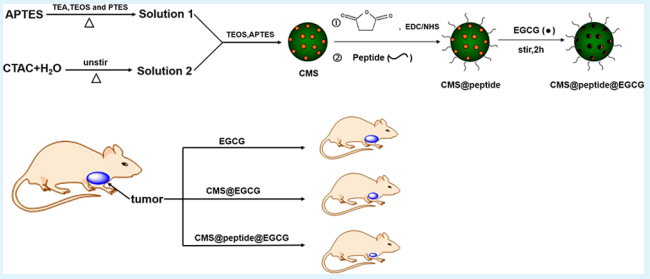


**KEYWORDS:** *(-)-epigallocatechin-3-gallate, PEGA-pVEC peptide, targeted therapy, colloidal mesoporous silica, drug delivery system*

## INTRODUCTION

Chemotherapy is a method for cancer treatment in which the drugs are circulated throughout the entire body through the blood vessels and have influences on all of the body cells. However, this treatment is sometimes referred to as "cytotoxic therapy" because the used drugs can induce cell damage, including to cancer cells and to normal cells. Thus, researchers urgently seek a type of drug that only induces cancer cells apoptosis without damaging normal cells. One enticing drug is (-)-epigallocatechin-3-gallate (EGCG), since EGCG has a strong anticancer effect,[1−3] anti-HIV effects,[4] neuroprotective effects,[5] and DNA-protective effects.[6] It has been suggested that EGCG suppresses tumor promotion by inhibiting the release of tumor necrosis factor-alpha, which is believed to stimulate tumor promotion and progression of initiated cells as well as premalignant cells.[7−10] Therefore, some scientists believe that EGCG could be one of the most powerful anticancer compounds ever discovered. But according to previous studies, we have known that EGCG has some disadvantages in the application in the living body, such as poor liposolubility, rapid decomposition, low bioavailability, and shorter half-life.[11] Consequently, although EGCG as an anticancer drug has been applied to multicell lines,[12−14] the successful application of the drug to an animal model has been rare.[15] For overcoming those drawbacks of EGCG *in vivo*, it is hypothesized that EGCG loaded by drug carriers can promote the targeted aggregation and release of EGCG in tumor-bearing mice.

Colloidal mesoporous silica (CMS) as a kind of excellent inorganic carrier had aroused great interest in biomedical application, especially for cancer therapy. Compared with other

**Received:** June 24, 2015
**Accepted:** July 30, 2015
**Published:** July 30, 2015





DOI: 10.1021/acsami.5b05618
*ACS Appl. Mater. Interfaces* 2015, 7, 18145−18155

organic or macromolecular polymer carries, their unique physicochemical stability and a number of favorable structural features endow them with fascinating performances as an intelligent drug delivery system (DDS).[16−20] CMS with hollow and mesoporous structure could selectively and efficiently accommodate drug molecules.[21−23] In addition, CMS with suitable size can effectively accumulate in the cancer cells and tumors *in vivo* via an enhanced permeability and retention (EPR) effect. In previous research, we have demonstrated that CMS is capable of loading EGCG by electrostatic attraction to increase the anticancer ability of EGCG *in vitro*;[24] however, there have been no reports for cancer therapy *in vivo*. This is because the physiological environment of the animal model is sufficiently complicated that the study results *in vitro* and *in vivo* are not entirely consistent.[25,26] The following three aspects need to be considered if CMS DDS applies *in vivo*: (1) escaping the capture of the immune system to let drugs through a series of biological barriers, (2) improving the efficacy of treatment by transferring the drug to specific tissues, and (3) increasing the pharmacological properties of the drug without changing the structure of drug molecules. Although CMS had been applied to the load and release of anticancer drug via the EPR effect *in vivo*,[27−29] target ligands need to be modified on the surface of CMS for the selective and specific release of drug in certain tumors.

Antibody, peptide, and aptamer are major cancer-specific targeting ligands which can distinguish different tumor types and various stages of tumor development.[30−32] However, an important factor for drug delivery is the efficient passage of drugs or drug-carriers through the plasma membrane. Improving the translocation process of drugs or carriers across the plasma membrane has some advantages, such as significantly reducing the quantity of drug to be administered, prolonging the half-life of the anticancer drug, and diminishing the side effects on healthy tissues. With the purpose of providing a cell-penetrated and targeted vector, Myrberg designed a tumor-homing cell-penetrating peptide, named PEGA-pVEC peptide, which is taken up by breast cancer cells *in vitro* and internalized *in vivo* by accumulating in blood vessels in breast tumor tissue.[33] Accordingly, the PEGA-pVEC peptide is conjugated on the surface of CMS and CMS@peptide, which can be useful in the induction and accumulation of CMS to an intracellular location in breast tumor target tissue.

Here, to MCF-7 breast cancer as the target object *in vivo*, we designed a highly selective and versatile CMS DDS. The DDS was fabricated using PEGA-pVEC peptide modified on the surface of CMS via aminoxatyl reaction and EGCG loaded into the interstitial hollow space of CMS by electrostatic interaction. We engineered that peptide accumulated CMS@EGCG into breast vasculature and tumor, which displayed a more effective and specific guidance for EGCG delivery *in vivo*; EGCG was released from CMS and exhibited a strong inhibition action to the growth of breast tumor. Through *in vitro* study of MCF-7 cells and *in vivo* detection of the marine MCF-7 xenograft nude mice, we have proved that drug loading by CMS@peptide could dramatically enhanced the therapeutic efficacy of EGCG.

## EXPERIMENTAL SECTION

**Materials.** (3-Aminopropyl)triethoxysilane (APTES), triethanolamine (TEA), tetraethyl orthosilicate (TEOS), cetyltrimethylammonium chloride (CTAC), phenyltriethoxysilane (PTES), 1-Ethyl-3-(3-dimethyllaminopropyl)carbodiimide hydrochloride (EDC), *N*-hydroxysuccinimide (NHS), (-)-epigallocatechin gallateand (EGCG, 95%) and succinic anhydride were obtained from Sigma-Aldrich. Peptides (cCPGPEGAGC-LLIILRRRIRKQAHAHSK-NH2) were synthesized by Life technologies. 1640 medium and fetal bovine serum (FBS) were purchased from Gibco. Acrylamide, tris(hydroxymethyl)-aminomethane (Tris), sodium dodecyl sulfate (SDS), ammonium persulfate (APS), tetramethylethylenediamine (TEMED), dithiothreitol (DDT), glycine (Gly), hydrochloric acid (36%) and bromophenol blue (BPB) were from Sinopharm Chemical Reagent Co., Ltd. Yili skimmed milk powder was bought from super market. CCK-8 kit and Hoechst 33258 were purchased from Dojindo Molecular Technologies, Inc. Allophycocyanin (APC), Propidium Iodide (PI), Caspase-3 kit, ROS Fluorescent Probe-DHE, BSA kit and MCF-7 cells were obtained from KeyGEN BioTECH. Ddwater was used in all experiments. All chemicals were used as received without further purification.

**Synthesis and Characterization of CMS.** The synthesis of CMS based on Bein.[30] In order to get a good EPR, the size of CMS was controlled about 80 nm. 14.3 g of TEA, 1.557 g of TEOS and 110.8 mg of PTES were mixed and heated to 90 °C for 20 min without stirring. The reaction product was named solution 1. A preheated mixture of CTAC (2.41 mL) and 21.7 g of $ddH_2O$ (solution 2) at 60 °C were added to solution 1 and stirred at 500 rpm for 20 min. Next 183.2 mg of TEOS was added at one time with a continued stirring for another 40 min. After that time, TEOS (18.32 mg) and APTES (16.53 mg) was added and stirred overnight at room temperature. The products were collected by centrifugation, washed three times with ethanol, and redispersed. To extract the organic template from the mesoporous silica nanoparticles, the suspension obtained above was dispersed in a solution containing 2 g of ammonium nitrate in absolute ethanol (100 mL) and refluxed at 90 °C for 45 min. The final product was separated by centrifugation and dispersed in ethanol.

The morphology of CMS were recorded on a JEOL-2010 TEM at acceleration voltage of 200 kV (JEOL, Japan). Zeta-potentials were performed on a Malvern Nano-z ZETA potentiostat.

**Preparation of CMS@peptide, CMS@EGCG and CMS@peptide@EGCG.** Three mg of CMS and 1.5 mg of succinic anhydride were dispersed in *N*,*N*-dimethylformamide and stirred overnight. Then the products were purified by centrifugation to remove the excess succinic anhydride. The deposition was ultrasonically dispersed in PBS (pH = 5.3). Next, 28.75 mg of EDC and 43.15 mg of NHS were added to activate the carboxyl for 20 min, washed and dispersed in PBS (pH = 7.4). In order to achieve the target of CMS to special cancer cells and tumor, 1 mL of peptide (1 mg/mL) was added and stirred for 4 h. The product was named CMS@peptide.

One milligram of CMS or CMS@peptide was mixed with 1 mL of EGCG solution in PBS (1 mg/mL), respectively. After being stirred for 2 h in the dark, the EGCG-loaded particles were collected by centrifugation, named CMS@EGCG and CMS@peptide@EGCG.

***In Vitro* Drug Release.** Each of the above-prepared CMS@EGCG (1 mg) and CMS@peptide@EGCG (1 mg) in a 10000 Ka dialysis bag was immersed in 20 mL pH 7.4 or 5.0 PBS, with stirring at room temperature. At certain time intervals, 8 mL of the release medium were taken out to test the concentration of EGCG by UV/vis spectroscopy measurements at a wavelength of 325 nm and then was returned to the original PBS. The absorbance of supernatant PBS were recorded on a Nanodrop-2000C micro UV−vis spectrophotometer.

**Cell Culture.** MCF-7 cells were seeded in 10 cm culture dishes with 1640 containing 10% FBS and 5% penicillin-streptomycin at 37 °C in a 5% $CO_2$ humidified environment. After the cell concentration reached 80%, the next cell experiments could be done. Then, cells were seeded in 96-well culture plate for the CCK-8 assay. Cells were stained with APC-PI in 6-well culture plate for Flow cytometry, and 35 mm glass bottom dishes were used for confocal image by using a TCS SP5 Confocal Laser Microscope (Leica, Germany).

**Cytotoxicity Assessment.** MCF-7 cells were seeded at a concentration of 5000 cells/well in 96-well culture plate. After culturing for 24 h, complete medium was replaced with serum free medium for another 24 h. Then, CMS, EGCG, CMS@EGCG and CMS@peptide@EGCG was dispersed in complete medium with different concentrations of 5, 10, 20, 40, 60, 80, 100, 120, and 150 μg


DOI: 10.1021/acsami.5b05618
ACS Appl. Mater. Interfaces 2015, 7, 18145−18155

**Scheme 1. (a) Design of the Targeting Drug Delivery System, and (b) Schematic Diagram of the Therapy Effect of EGCG, CMS@EGCG, and CMS@peptide@EGCG *in Vivo***

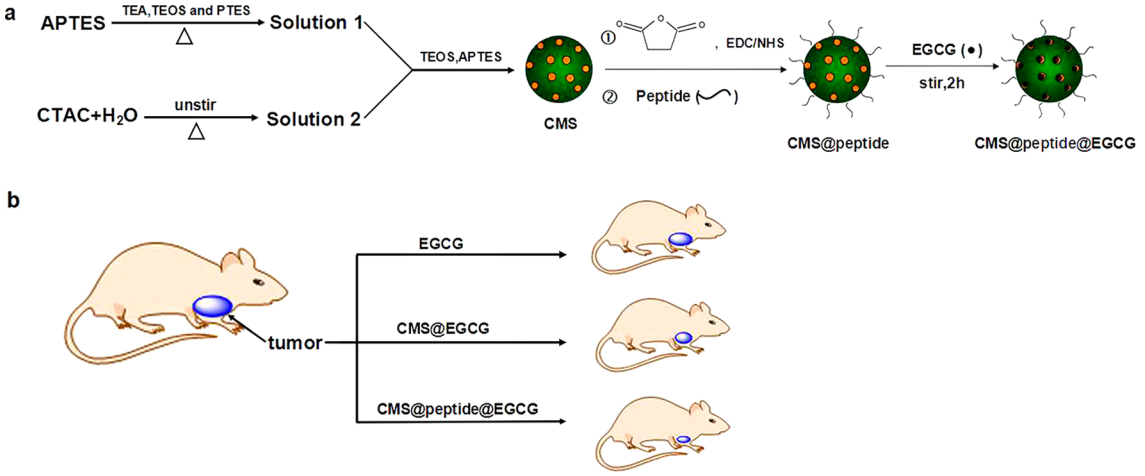


of EGCG/ml and added to the wells for 24/48/72 h. The cell cytotoxicity *in vitro* was measured by CCK-8 assay. The inhibition ratio was calculated using $1\text{-}OD_{sample}/OD_{control}$.

**Flow Cytometry.** For evaluating cell apoptosis, flow cytometry was performed using an APC-PI apoptosis detection kit. After treatments with 60 or 100 $\mu$g of EGCG/ml of EGCG, CMS@EGCG and CMS@peptide@EGCG, cells were detached by incubation with 0.25% trypsin for 5 min and centrifuged at 1000 rpm for 5 min, then washed by cool PBS twice. The cells were resuspended in 600 $\mu$L of PBS including APC-PI (20 $\mu$g/mL) and incubated for 30 min at 4 °C in the dark. Cells were assayed by FACSCanto II flow cytometry (Becton, Dickinson and Company, USA).

**Enhanced Cellular Uptake *in Vitro*.** MCF-7 cells were seeded at a density of $10^5$ cell/well in glass bottom dishes and incubated for 24 h at 37 °C under 5% $CO_2$. Then, EGCG, CMS@EGCG and CMS@peptide@EGCG were dispersed into 1640 cell culture medium with a concentration of 60 or 100 $\mu$g of EGCG/ml and replaced original medium in the culture dishes. Twenty-four hours after incubation, the cells were washed three times with PBS to remove the nonuptake materials followed by nuclei staining with Hoechst 33258. The confocal fluorescence imaging were performed on TCS SP5 Confocal Laser Microscope (Leica, Germany) equipped with an ultraviolet laser, while Hoechst 33258 was excited with 350 nm light. Luminescence signals were detected in the wavelength regions of 400−500 nm.

**Confocal Imaging of CMS@FITC/CMS@FITC@peptide and ROS Fluorescent Probe-DHE.** After the MCF-7 cells were incubated with CMS@FITC and CMS@FITC@peptide of 30 $\mu$g/mL for 4h to perform the fluorescence detection of FITC and PI with confocal microscopy. FITC was excited at 488 nm with an argon ion laser, and the emission was collected at 485−550 nm. PI was excited at 535 nm with an argon ion laser, and the emission was collected at 590−640 nm.

The EGCG-induced generation of ROS was also examined. After the cells were incubated with CMS, EGCG, CMS@EGCG, CMS@peptide@EGCG of 60 $\mu$g/mL to EGCG for 4 h, the cells were stained with DHE and DAPI to visualize the generation of ROS with confocal laser scanning microscope. DHE was excited at 488 nm with an argon ion laser, and the emission was collected from 590 to 610 nm. DAPI was excited at 360 nm with an argon ion laser, and the emission was collected from 440 to 480 nm. All images were digitized and analyzed by Leica Application Suite Advanced Fluorescence (LAS-AF) software.

**Caspase-3 Activity Assay.** The Caspase-3 activity kit was used to evaluate the activity of caspase-3. The absorption was measured by nanodrop at the wavelength of 405 nm. Results are presented as relative values compared to control.

**Western Blotting.** MCF-7 cells were incubated with 60 or 100 $\mu$g of EGCG/ml of EGCG, CMS@EGCG and CMS@peptide@EGCG for 24h, washed three times with PBS and suspended in 100 $\mu$L of lysis buffer. Protein concentration was determined by BCA assay. Twenty $\mu$g of total protein was boiled for 5 min in 4.5 $\mu$L of SDS sample buffer. The equal amount of proteins was loaded in each lane of 10% (w/v) SDS-polyacrylamide gel electrophoresis (SDS-PAGE) and then electrically transferred to a nitrocellulose membrane (NC membrane). After blocking the membranes with 5% (w/v) skimmed milk for 2 h, target proteins were immunoblotted with PARP, anti-P-ERK, anti-P-MSK, and Bcl-xl antibodies at 4 °C overnight. This was followed by binding of horseradish peroxidase (HRP)-conjugated antirabbit IgG (secondary antibody) and signal detection with an enhanced chemiluminescent substrate.

***In Vivo* Anticancer.** All animal experiments were in agreement with the guidelines of the Institutional Animal Care and Use Committee. Tumor-bearing Female Balb/c nude mice with average weight of 20 g (8−10 weeks) were purchased from KeyGEN BioTECH. When the tumor volume reached 50 $mm^3$, the animals were treated with each formulation.

The mice were randomly divided into five groups (six mice per group): (1) saline control, (2) blank nanoparticles, (3) free EGCG, (4) CMS@EGCG, and (5) CMS@peptide@EGCG. Corresponding group was injected 200 $\mu$L of solution of neat saline, CMS dispersed in saline, free EGCG, CMS@EGCG, and CMS@peptide@EGCG (at a dose normalized to be 100 mg/kg EGCG equiv), respectively, via tail vein. Each formulation was injected five times at 3-day intervals (days 0, 3, 6, 9, 12, and 15). Total mice were euthanized at 18 d post treatment, and tumor tissues of the above-mentioned treatment groups were harvested for histological study by hematoxylin-eosin (H&E) staining under a BX51 optical microscope (Olympus, Japan) in a blinded fashion by a pathologist. Tumors volumes were measured and the mice were weighted every 3 days. The relative tumor volumes were calculated for each mouse as $V/V_0$ ($V_0$ was the tumor volume when the treatment was initiated).

**Histological Analysis.** For histological studies, the samples of brain, lung, liver, spleen, kidney, small intestines and heart were fixed in 10% neutral buffered formalin. Then they were embedded in paraffin and cut into approximately 4 $\mu$m thick section, and stained with hematoxylin and eosin (H&E). The histological sections were observed under an optical microscopy.

## RESULTS AND DISCUSSION

**Characterization of CMS and CMS@peptide.** The synthetic approach of CMS was summarized in Scheme 1a.[34] First, triethanolamine (TEA), tetraethyl orthosilicate (TEOS), and phenyltriethoxysilane (PTES) were mixed followed by heating for 20 min at 90 °C without stirring, named solution 1. Solution 2 was composed of CTAC and water and preheated at 60 °C. Subsequently, solution 2 was added to solution 1 and


DOI: 10.1021/acsami.5b05618
ACS Appl. Mater. Interfaces 2015, 7, 18145−18155

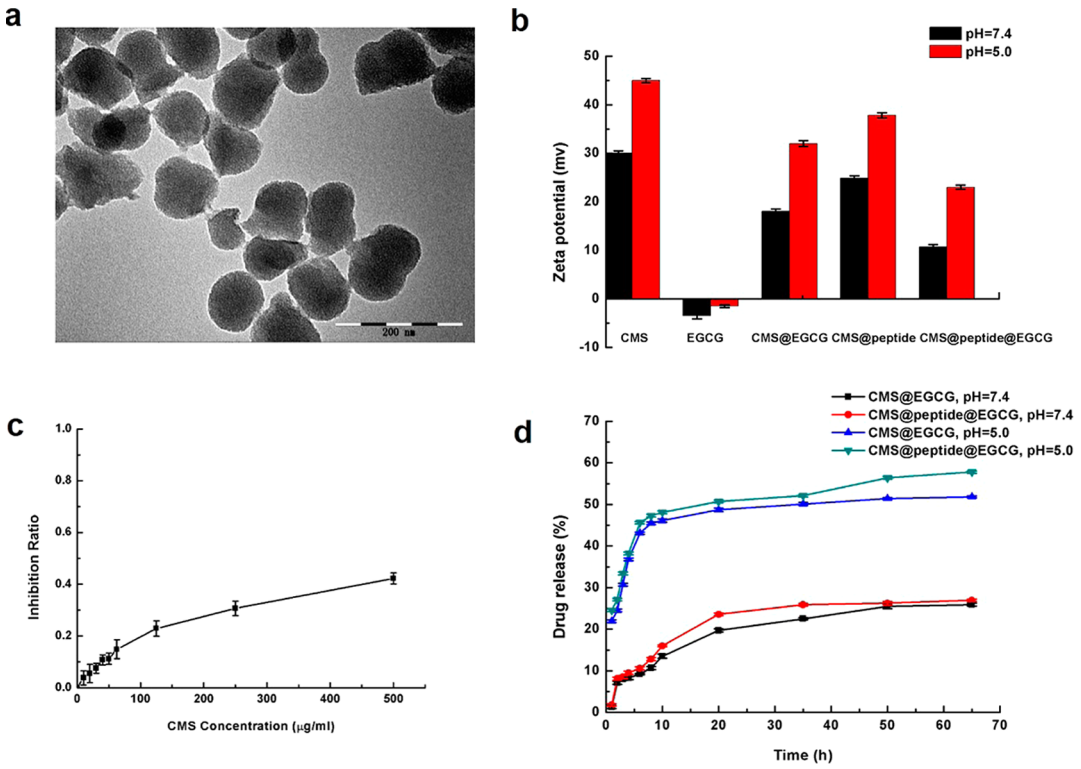


**Figure 1.** (a) TEM image of CMS with a size of 80 nm, (b) zeta potential of CMS, EGCG, CMS@EGCG, CMS@peptide, and CMS@peptide@EGCG in pH = 7.4 or 5.0 PBS, (c) inhibition ratio with concentrations of CMS from 5 $\mu$g/mL to 500 $\mu$g/mL for 24 h, (d) *in vitro* drug release of EGCG from CMS and CMS@peptide in pH = 7.4 PBS medium at room temperature.

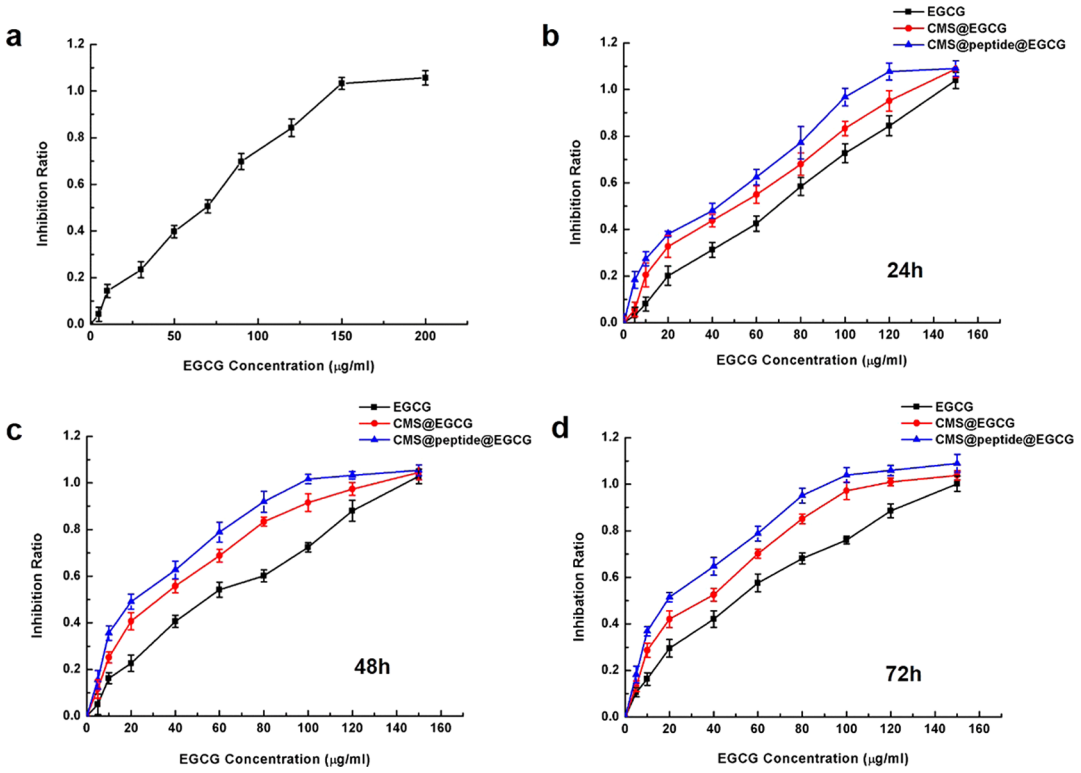


**Figure 2.** Cytotoxicity of EGCG (a) and of (b, c, d) EGCG, CMS@EGCG, and CMS@peptide@EGCG on MCF-7 cells by CCK-8 assays for 24 h, 48 h, and 72 h (b, c, d).

stirred for 20 min. Next to the reaction product was added enough CTAC, and the reaction mixture was stirred for another 40 min. Last, the mixture of TEOS and (3-aminopropyl)-trimethoxysilane (APTES) was added and stirred overnight at room temperature. The final product was CMS, with the outer surface modified with amino. The transmission electron



DOI: 10.1021/acsami.5b05618
*ACS Appl. Mater. Interfaces* 2015, 7, 18145−18155

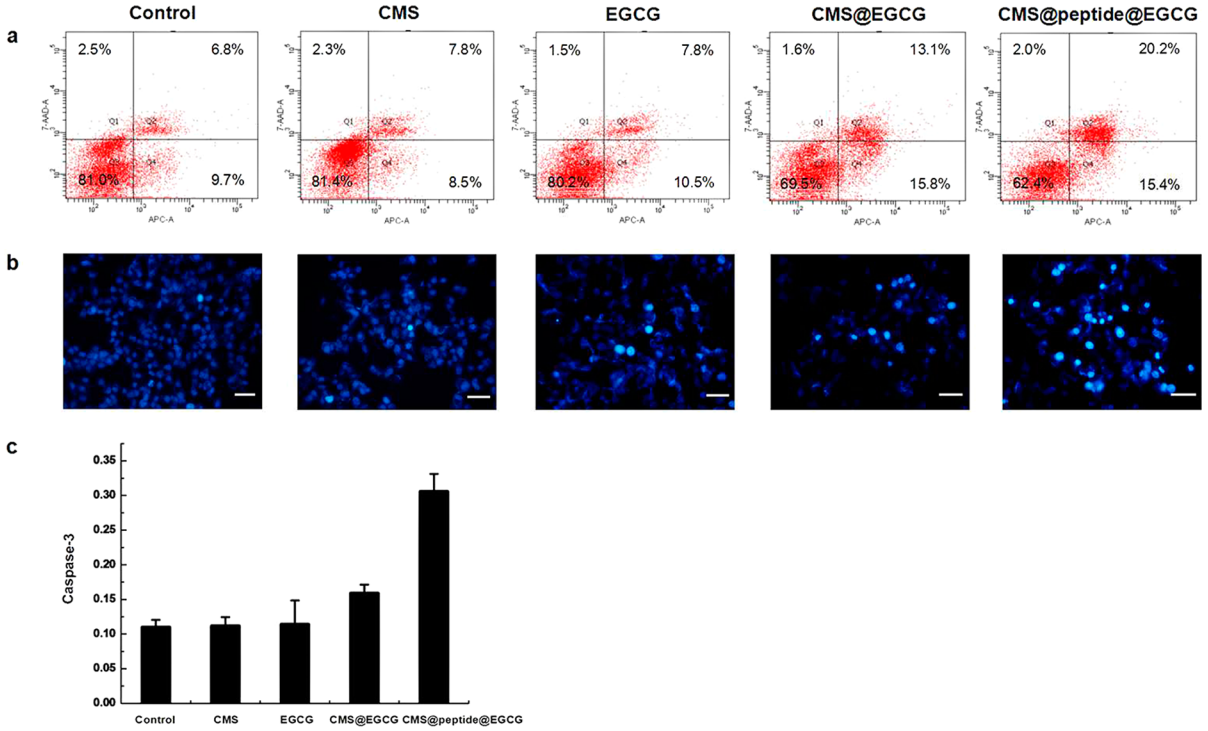


**Figure 3.** (a) Flow cytometric analysis of MCF-7 cell death induced by CMS, free EGCG, CMS@EGCG, and CMS@peptide@EGCG at the equivalent EGCG concentration (60 $\mu$g/mL) for 24 h. Flow cytometry profile represented APC staining on the X axis and PI on the Y axis. (b) Cell imaging visualized the changes of the nucleus when cells were treated by CMS, CMS@EGCG, and CMS@peptide@EGCG. Nucleus stained with Hoechst 33258. (c) Activity of capase-3 in cells treated with CMS, free EGCG, CMS@EGCG, and CMS@peptide@EGCG.

microscopy (TEM) image (Figure 1a) shows CMS with a moderate size of 80 nm and evidence for the mesoporous and nonaggregated nature. The hydrodynamic diameter of the CMS was 85 nm (Figure S1a, Supporting Information), which was close to the size measured by TEM. The modification of peptide on the surface of CMS could increase the size of particles to ~100 nm (Figure S1b, Supporting Information). After CMS or CMS@peptide had been dispersed in complete medium for some time (0−5 day), the hydrodynamic diameters of two kinds of particles increased to ~150 or 180 nm because of electrostatic adsorption of proteins in serum (Figure S1c, Supporting Information). The localization of the aminopropyl groups in the shell of CMS endowed a surface with high positive charge. Based on the zeta potential of CMS and EGCG, EGCG was loaded on CMS by electrostatic attraction (Figure 1b). To evaluate the biocompatibility of CMS, MCF-7 cells were incubated with different concentrations of CMS for 24 h. Figure 1c showed the CMS had no obvious adverse effect on cell viability within the tested concentration range, even as high as 200 $\mu$g/mL, demonstrating the CMS itself had no cytotoxicity. Figure 1d exhibited the drug release profiles in pH = 7.4 or 5.0 PBS, replacing medium at different time intervals. In pH 7.4 PBS buffer, it could be seen that no more than 20% of EGCG released from CMS@EGCG in 20 h, while about 23% of the release amount was achieved in CMS@peptide@EGCG. Beyond 20 h, the drug releases tended to a balance; less than 6% of EGCG released in the last 45 h. But when the pH value was reduced to 5.0, the drug release rate rapidly reached to 21.9% in 1 h. The major reason for EGCG released from CMS was the change of electrostatic interaction between positively charged CMS and negatively charged EGCG molecule in buffer solution. When peptide was modified, the zeta potential value of CMS decreased. So CMS@peptide@EGCG exhibited higher release rate than CMS@EGCG under the same conditions. Under the acidic microenvironment of solid tumor growth, the speed of EGCG released was increased, and the local concentration of EGCG in tumor was improved.

**Cytotoxicity of EGCG, CMS@EGCG, and CMS@peptide@EGCG.** Next, the cytotoxicity of free EGCG, CMS@EGCG, and CMS@peptide@EGCG to MCF-7 cells was evaluated at different concentrations and for distinct incubation time via the CCK-8 assay. From Figure 2, it could be seen that all of them showed obvious cytotoxicity, which became more significant following the increase of EGCG concentrations and incubation time. The three samples showed distinct cell inhibition at the three time points (24, 48, or 72 h), with EGCG concentration from 5 to 150 $\mu$g/mL. With prolonged incubation time, the cytotoxicity of CMS@EGCG and CMS@peptide@EGCG was higher than that of free EGCG under the same conditions. When the cells were incubated for 24 h, the inhibition ratio of CMS@peptide@EGCG approximately reached 100%, corresponding to the concentration of EGCG of 100 $\mu$g/mL. Such an increasingly amplified cytotoxicity by CMS@EGCG and CMS@peptide@EGCG was generally attributed to two factors: the EPR effect of CMS and the targeting and cell-penetration of PEGA-pVEC peptide to MCF-7 cells.

To further demonstrate the action of drug carriers reinforcing the anticancer effect of EGCG, MCF-7 cells treated with free EGCG, CMS@EGCG, and CMS@peptide@EGCG were evaluated and compared by flow cytometry and Hoechst 33258 staining. In Figure 3a, CMS exhibited negligible cytotoxicity against MCF-7 cells compared with blank control, in accordance with the above-mentioned CCK-8 assay. However, an apparent toxic effect of EGCG could be identified to be 1.5% of cell necrosis, 7.8% of cell apoptosis, and 10.5% of


DOI: 10.1021/acsami.5b05618
ACS Appl. Mater. Interfaces 2015, 7, 18145−18155

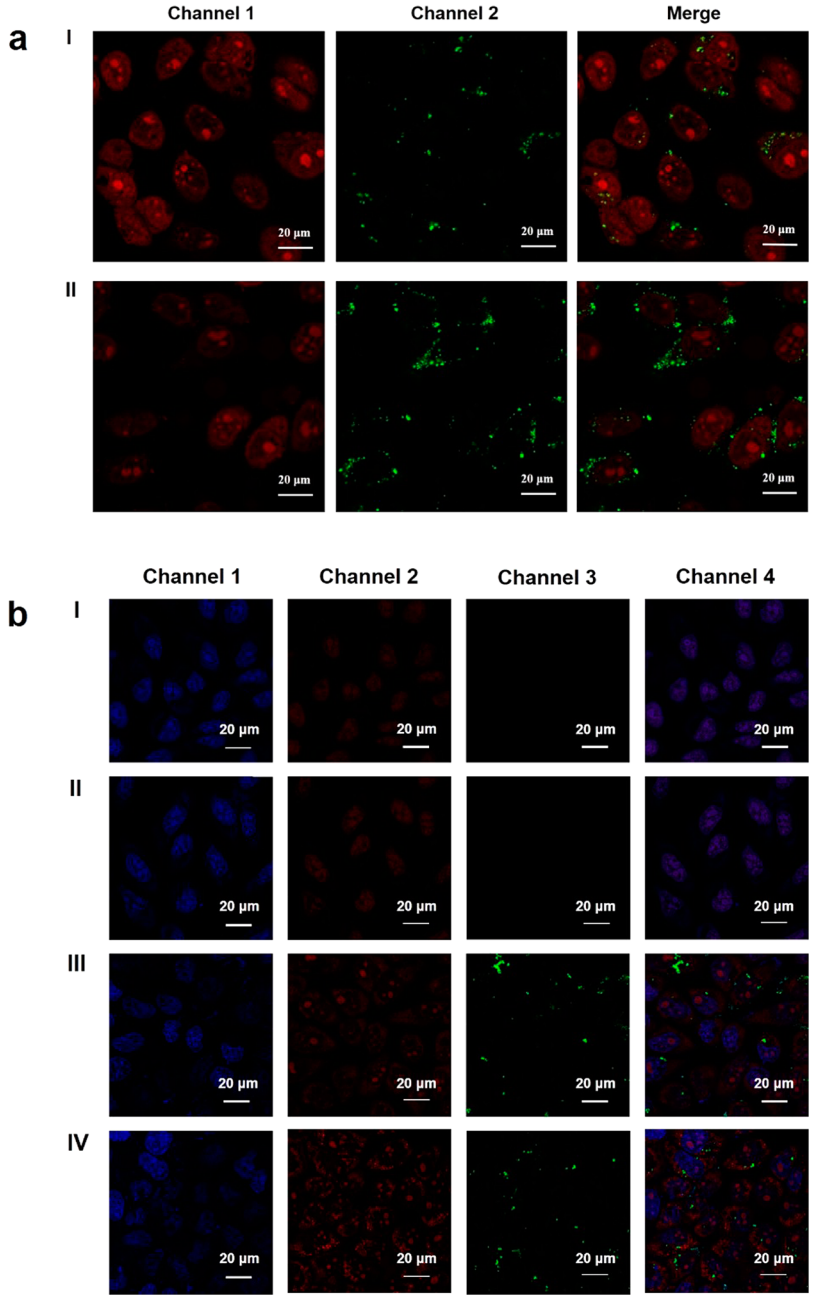


**Figure 4.** (a) Confocal microscopy images of MCF-7 cells following treatment of CMS (I) and CMS@peptide (II) for 4 h. The concentration of CMS was 30 μg/mL. The green fluorescence came from FITC which was trapped in the core of CMS. Nuclei were stained with PI. (b) The MCF-7 cells were incubated by EGCG (II), CMS@EGCG (III), and CMS@peptide@EGCG (IV) of 60 μg/mL to EGCG for 4 h. The fluorescence of blue, red, and green came from DAPI, DHE, and FITC, respectively.

early apoptosis at the EGCG concentration of 60 μg/mL, suggesting that the cytotoxicity of EGCG was mainly related to the apoptosis-related cell death. By comparison, CMS@EGCG demonstrated a greatly improved cell apoptosis up to 13.1% and slightly enhanced cellular early apoptosis to 15.8%, corresponding to 60 μg/mL of free EGCG. Even so, the modification of peptide on CMS further improved the apoptosis of MCF-7 cells, whose cell apoptosis reached to 20.2%, incubating cells with EGCG of the same concentration as CMS@EGCG. When the concentration of EGCG was 100 μg/mL, we could see the same trend in Figure S2a and Table S1 (Supporting Information). These results indicated that incorporating EGCG into CMS or CMS@peptide would enhance the apoptosis ratio of cells, with no influence to the pathway of apoptosis.

To further verify the result of flow cytometry, the MCF-7 cells were incubated with EGCG, CMS@EGCG, and CMS@peptide@EGCG with concentration of EGCG at 60 μg/mL for 24 h, fixed with 4% paraformaldehyde, and then stained with Hoechst 33258 (Figure 3b). Chromatin condensation and apoptotic body formation could be observed for most of the cells treated with EGCG, CMS@EGCG, and CMS@peptide@EGCG. Following the increase in the proportion of bright blue cells, CMS@peptide@EGCG exhibited the strongest pro-apoptotic ability to MCF-7 cells. No visible apoptosis was observed of the cells treated with CMS (5 μg/mL, experimental


DOI: 10.1021/acsami.5b05618
ACS Appl. Mater. Interfaces 2015, 7, 18145−18155

concentration) and control cells. In Figure S2b (Supporting Information), the concentration of EGCG was 100 μg/mL, which showed the same consequence with 60 μg/mL of EGCG. Furthermore, we had examined the level of a key DAMP biomarker, capase-3, to evaluate apoptosis (Figure 3c and S1c, Supporting Information). The results indicated that the relative value of capase-3 was indeed enhanced by the loading of EGCG within CMS and CMS@peptide, compared with free EGCG, further confirming the reliability of flow cytometry and Hoechst 33258 staining.

**Modification of Peptide on the Surface of CMS.** Tumor-homing cell-penetrating peptide was modified to promote CMS and EGCG enriched in the cells. The characteristic peaks of peptide occurred in Fourier transform infrared (FT-IR, Figure S3, Supporting Information), which proved the formation of CMS@peptide. Fluorescent dye, FITC, was trapped in the core of CMS, which could indicate the position and amount of CMS in cells. From the results of confocal imaging (Figure 4a), we could see that the fluorescence intensity of CMS@peptide is significantly stronger than that of CMS.

EGCG possesses a strong anticancer effect because it can produce reactive oxygen species (ROS). After treatment of MCF-7 cells with EGCG, CMS@EGCG, and CMS@peptide@EGCG in the same concentration of EGCG, cells were stained with ROS fluorescence probe (Dihydroethidium, DHE) to ensure the amount of ROS. In Figure 4b, the red fluorescence of DHE had become noticeably stronger with the loading of EGCG by CMS and CMS@peptide. The EPR effect of CMS and the targeting of peptide were responsible for the enhancement of EGCG concentration in cells. The above results demonstrated that peptide could effectively increase the enrichment of EGCG and CMS in cells.

**Gene Expression Analysis.** To verify whether the apoptosis-corresponding proteins had the same tendency of regulations with the flow cytometry, Western blot analysis (WB) was used to measure the expressions of corresponding proteins, as shown in Figure 5. Poly ADP-ribose polymerase (PARP) is a cleavage substrate of caspases which plays an important role in DNA damage repair and apoptosis. Anticancer drugs could induce the cleavage of PARP to form two separate pieces of the band in WB. CMS@peptide@EGCG treatment caused more robust PARP cleavage than EGCG and CMS@EGCG in MCF-7 cells (Figure 5).

Mitogon activated protein kinase (MAPK) signaling transduction is a key pathway of cellular proliferation and apoptosis regulation. Early respondent kinases (ERK) is a member of the MAPK family which is closely associated with a variety of abnormal tumor development. Thus, some part of the cascade pathways of this signaling channel has the anticancer effect, in theory. The rough mode of ERK signaling transduction is from a variety of growth factors, from Ras to Raf to MSK to cell growth, development, division, and differentiation in which MSK is the downstream target molecule of ERK. In the total physiological process, ERK and MSK are activated to P-ERK and P-MSK. It could be seen from Figure 5 that P-ERK and P-MSK shared a similar tendency of regulation by CMS, free EGCG, CMS@EGCG, and CMS@peptide@EGCG.

To investigate the molecular mechanism of CMS and CMS@peptide, improving the anticancer effect of EGCG, we examined the expression of Bcl-xl in WB. Bcl-xL is the member of Bcl-2 family proteins which plays an important role in the regulation of apoptosis. Bcl-xL could combine with pro-

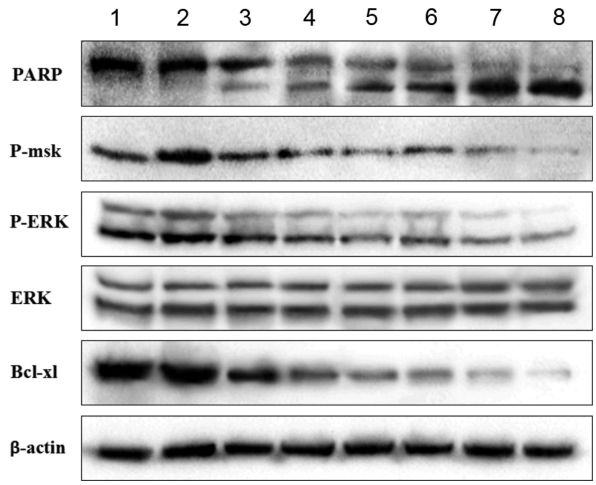


**Figure 5.** Western blotting analysis results of apoptosis related proteins, PARP, P-ERK, P-MSK, and Bcl-xl in the prepared cell extracts after 24 h of treatment. Equal loading was confirmed by reprobing the blot for ERK-total and β-actin proteins. (1) Control, (2) 30 μg/mL CMS, (3) 60 μg/mL EGCG, (4) CMS@EGCG of 60 μg/mL EGCG, (5) CMS@peptide@EGCG of 60 μg/mL EGCG, (6) 100 μg/mL EGCG, (7) CMS@EGCG of 100 μg/mL EGCG, (8) CMS@peptide@EGCG of 100 μg/mL EGCG.

apoptotic proteins to form heterodimers and inhibit apoptosis. In Figure 5, the WB results of Bcl-xl proved that CMS and CMS@peptide could effectively improve the inhibition of anticancer drugs.

The two following approaches were proposed for the highly inhibited ERK signaling transduction pathway by CMS@peptide@EGCG: (1) the EPR effect of nanoparticles intensified the concentration of EGCG in cells; (2) as above-mentioned, the conjugation of peptide on the surface of CMS, induced CMS, and EGCG targeted accumulation in cells, which in return aggravated the cell death. In conclusion, CMS@peptide@EGCG could more aggravate cell death compared with CMS@EGCG or free EGCG.

**Toxicity of CMS and Cancer Treatment of Drug *in Vivo*.** The therapeutic efficacy was assessed using the MCF-7 subcutaneous model. Scheme 1b described the trend of tumor size. The mice inoculated with tumor cells were randomly divided into five experimental groups, (a) control group (physiological saline), (b) CMS group (30 mg/kg CMS), (c) EGCG group (100 mg/kg of EGCG), (d) CMS@EGCG group (100 mg/kg of EGCG), and (e) CMS@peptide@EGCG (100 mg/kg of EGCG) with minimal weight and tumor size difference. The drugs were intravenously administered every 3 days (day 0, day 3, day 6, day 9, day 12, and day 15) for a total of six times. No mice died during the course of therapy. Then, to the day of the end point, all of the animals were sacrificed to evaluate the tumor sizes and weights. The picture of mice and tumors (Figure 6a) showed that the tumor sizes of the CMS@peptide@EGCG group were visibly the smallest in all experimental groups. The average inhibition rate calculated from tumor weights by comparison of EGCG group or CMS@EGCG group to control group was about 69.9% or 80.58%, while that of the CMS@peptide@EGCG group was as high as 89.66% (Figure 6b).

The treatments were assessed by monitoring their relative tumor volumes during six treatment periods. After tail vein injection of samples, tumor growth was inhibited in all groups


DOI: 10.1021/acsami.5b05618
ACS Appl. Mater. Interfaces 2015, 7, 18145−18155

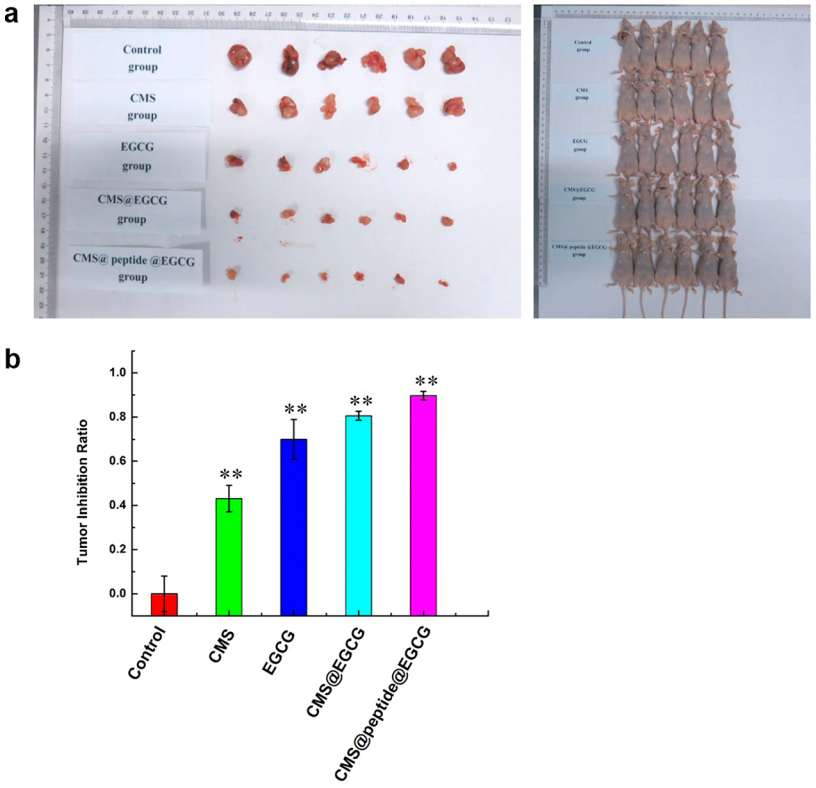


**Figure 6.** *In vivo* antitumor activities of CMS, free EGCG, CMS@EGCG, and CMS@peptide@EGCG on MCF-7 breast cancer subcutaneous model (30 mg/kg of CMS, 100 mg/kg of EGCG, five doses). (a) Photographs of female nude mice bearing breast cancer and stripped tumor tissues. (b) Tumor inhibition ratios were calculated using 1-weight$_{sample}$/weight$_{control}$.

(Figure 7a). The treatment efficacy in terms of tumor cell death was also evaluated by H&E staining on tissue sections from the different treatment groups at 18 days after treatment. Prominent necrosis was observed in histological sections from the groups treated by EGCG, CMS@EGCG, and CMS@peptide@EGCG (Figure 7b), indicating the successful destruction of the tumor cells by the load of EGCG with CMS and CMS@peptide. The tumor tissues treated with CMS alone showed indiscernible necrosis, revealing that CMS had scarce toxicity. For further demonstrating the mechanism of tumor inhibition, we extracted peptides from tumor tissues for WB analysis. In Figure S4 (Supporting Information), the trends of associated peptides are completely consistent with other experimental results.

The potential *in vivo* toxicity or side effect is always a great concern for anticancer drugs used in medicine. For verifying the practicability of EGCG and CMS, the mice were treated with EGCG at larger doses of CMS and CMS@peptide. The mice show significant body weight gain during 18 days after treatment (Figure S5, Supporting Information). After treatment, the major organs were thus collected for histology analysis. No noticeable sign of organ damage or tumor metastasis was observed from H&E stained organ slices (Figure 8), suggesting the negligible side effects of EGCG and CMS for cancer treatment *in vivo*.

Although breast cancer is a very stubborn disease, our results here proved that EGCG had an obvious treatment effect. The enhanced tumor inhibition of the CMS@peptide@EGCG may be attributed to the sustained release of EGCG from CMS@peptide *in vivo* when they were accumulated in the intratumor because of the EPR effect of the nanoparticle and targeting of the conjugated peptide. From the above results, it could been seen that the targeting of DDS for specific cancer cells and tumors could be endowed by further bioconjugating the CMS with tumor-homing cell-penetrating peptide.

## CONCLUSION

In summary, this study represents a significant progress of *in vivo* cancer therapy with a DDS in which the target molecule (peptide) is modified on the surface of CMS and EGCG is loaded in the pore. In previous research, we have demonstrated that CMSs themselves have excellent biocompatibility and cannot cause cytotoxicity *in vitro*. It is believed that further bioconjugating the CMS with tumor-homing cell-penetrating peptide would enhance the specific identification of the delivery system for certain cancer cells and cancers. Thus, breast cancer cells (MCF-7 cells) and MCF-7 tumor-bearing mice are chosen as the subjects to verify the performances of CMS and CMS@peptide *in vitro* and *in vivo*. The cell proliferation and apoptosis detection of MCF-7 cells reveal that further modified CMS with PEGA-pVEC peptide (CMS@peptide) is capable of significantly sensitizing EGCG to induce apoptosis of cancer cells in comparison with free EGCG and CMS@EGCG. In addition, EGCG reduces the change of apoptosis-related proteins which are not changed by CMS, indicating the possible synergies between the drug and the carrier in the CMS@peptide@EGCG and CMS@EGCG in inhibiting gene expression. Moreover, the CMS@peptide@EGCG shows a great therapeutic effect in MCF-7 tumor-bearing mice, exhibiting more excellent inhibiting ability to tumor growth as compared to CMS@EGCG and free EGCG. Meanwhile, no apparent *in vivo* side effects of the four experimental groups have been observed in toxicity studies by H&E stain, displaying


DOI: 10.1021/acsami.5b05618
*ACS Appl. Mater. Interfaces* 2015, 7, 18145−18155

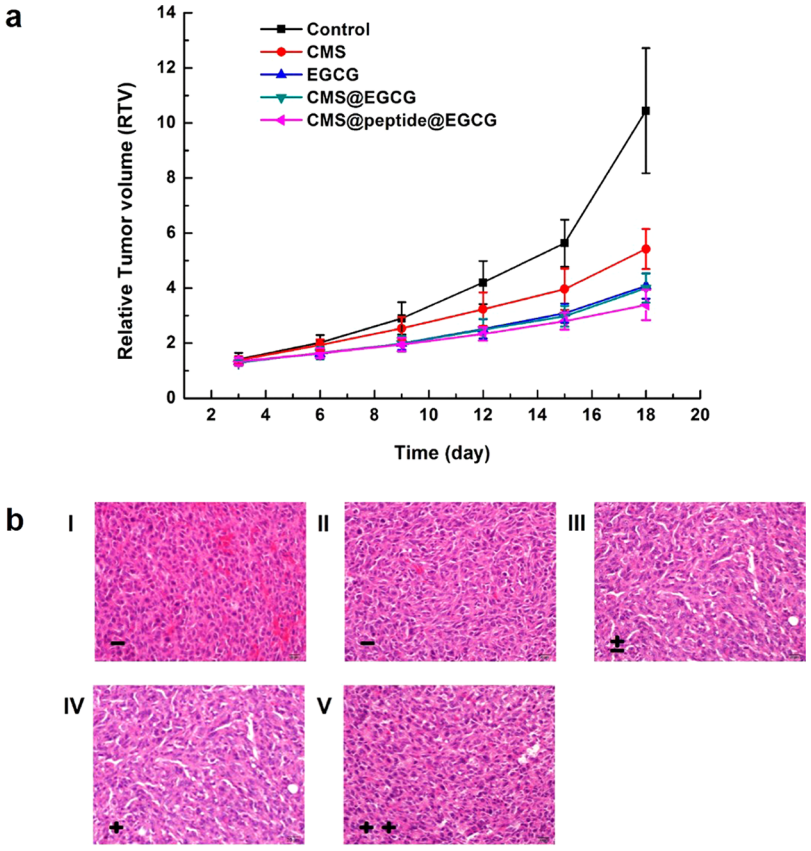


**Figure 7.** (a) Change of relative tumor volume ($V/V_0$) upon treatment with CMS, EGCG, CMS@EGCG, and CMS@peptide@EGCG for 18 days. Data are means ± SD (6 mice per group). (b) H&E staining of tumor tissue sections from different treatment groups at 18 days after treatment. ±: the degree of tissue injury.

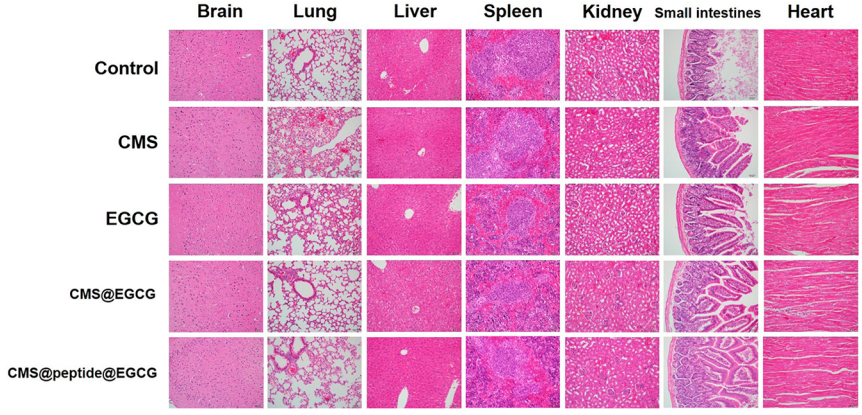


**Figure 8.** H&E stained images of tissue sections from different organs of mice with intravenous injection of CMS, EGCG, CMS@EGCG, and CMS@peptide@EGCG for 18 days.

good biocompatibility and no damage to normal tissue. Therefore, we anticipate that the present CMS@peptide will be highly attractive to enhance the efficacy of other anticancer drugs and pave the way for future targeting treatments.

## ■ ASSOCIATED CONTENT

### Supporting Information

The Supporting Information is available free of charge on the ACS Publications website at DOI: 10.1021/acsami.5b05618.

Additional experimental details, including DLS of CMS and CMS@peptide; the apoptosis experiments; the flow cytometric data; FT-IR spectra of CMS, CMS-peptide, and peptide; Western blotting analysis results of apoptosis related proteins from tumor tissues; and the weight changes of experimental mice during treatment (PDF)

## ■ AUTHOR INFORMATION

### Corresponding Authors

*E-mail: zhiweihe688@163.com.
*Telephone: (+86)769-2289-6219. Fax: (+86)769-2289-6175. E-mail: jjzhu@nju.edu.cn.



DOI: 10.1021/acsami.5b05618
ACS Appl. Mater. Interfaces 2015, 7, 18145−18155

### Notes

The authors declare no competing financial interest.

## ■ ACKNOWLEDGMENTS

This work was financially supported by Natural Science Foundation of China (Grant Nos. 81372137, 81201799, 21335004), Discipline construction funds (Molecular Biology of Cancer Team: Grant STIF201108), and Guangdong Medical College Science Founding (Grant No. XQ1202).

## ■ REFERENCES

(1) Wang, C. Z.; Mehendale, S. R.; Calway, T.; Yuan, C. S. Botanical Flavonoids on Coronary Heart Disease. *Am. J. Chin. Med.* **2011**, *39*, 661−671.
(2) Kumar, N.; Shibata, D.; Helm, J.; Coppola, D.; Malafa, M. Green Tea Polyphenols in the Prevention of Colon Cancer. *Front. Biosci., Landmark Ed.* **2007**, *12*, 2309−2315.
(3) Mak, J. C. Potential Role of Green Tea Catechins in Various Disease Therapies: Progress and Promise. *Clin. Exp. Pharmacol. Physiol.* **2012**, *39*, 265−273.
(4) Li, S.; Hattori, T.; Kodama, E. N. Epigallocatechin Gallate Inhibits the HIV Reverse Transcription Step. *Antivir Chem. Chemother* **2011**, *21*, 239−243.
(5) Yu, J.; Jia, Y.; Guo, Y.; Chang, G.; Duan, W.; Sun, M.; Li, B.; Li, C. Epigallocatechin-3-gallate Protects Motor Neurons and Regulates Glutamate Level. *FEBS Lett.* **2010**, *584*, 2921−2925.
(6) Morley, N.; Clifford, T.; Salter, L.; Campbell, S.; Gould, D.; Curnow, A. The Green Tea Polyphenol (-)-Epigallocatechin Gallate and Green Tea can Protect Human Cellular DNA from Ultraviolet and Visible Radiation Induced Damage. *Photodermatol., Photoimmunol. Photomed.* **2005**, *21*, 15−22.
(7) Du, G. J.; Wang, C. Z.; Qi, L.; Zhang, W. Z. Y.; Calway, T.; He, T. C.; Du, W.; Yuan, C. S. The Synergistic Apoptotic Interaction of Panaxadiol and Epigallocatechin Gallate in Human Colorectal Cancer Cells. *Phytother. Res.* **2013**, *27*, 272−277.
(8) Nakazato, T.; Ito, K.; Ikeda, Y.; Kizaki, M. Green Tea Component, Catechin, Induces Apoptosis of Human Malignant B cells via Production of Reactive Oxygen Species. *Clin. Cancer Res.* **2005**, *11*, 6040−6049.
(9) Lambert, J. D.; Elias, R. J. The Antioxidant and Pro-oxidant Activities of Green Tea Polyphenols: A role in Cancer Prevention. *Arch. Biochem. Biophys.* **2010**, *501*, 65−72.
(10) Fujiki, H.; Suganuma, M. Green Tea: An Effective Synergist with Anticancer Drugs for Tertiary Cancer Prevention. *Cancer Lett.* **2012**, *324*, 119−125.
(11) Carlson, J. R.; Bauer, B. A.; Vincent, A.; Limburg, P.; Wilson, J. T. Reading the Tea Leaves: Anticarcinogenic Properties of (-)-Epigallocatechin-3-Gallate. *Mayo Clin. Proc.* **2007**, *82*, 725−732.
(12) Hou, Z.; Sang, S. M.; You, H.; Lee, M.-J.; Hong, J.; Chin, K.-V.; Yang, C. S. Mechanism of Action of (-)-Epigallocatechin-3-Gallate: Auto-oxidation-Dependent Inactivation of Epidermal Growth Factor Receptor and Direct Effects on Growth Inhibition in Human Esophageal Cancer KYSE 150 Cells. *Cancer Res.* **2005**, *65*, 8049−8056.
(13) Hong, J.; Lu, H.; Meng, X. F.; Ryu, J.-H.; Hara, Y.; Yang, C. S. Stability, Cellular Uptake, Biotransformation, and Efflux of Tea Polyphenol (-)-Epigallocatechin-3-Gallate in HT-29 Human Colon Adenocarcinoma Cells. *Cancer Res.* **2002**, *62*, 7241−7246.
(14) Yang, C. S.; Wang, H. Mechanistic Issues Concerning Cancer Prevention by Tea Catechins. *Mol. Nutr. Food Res.* **2011**, *55*, 819−831.
(15) Chung, J. E.; Tan, S.; Gao, S. J.; Yongvongsoontorn, N.; Kim, S. H.; Lee, J. H.; Choi, H. S.; Yano, H.; Zhuo, L.; Kurisawa, M.; Ying, J. Y. Self-assembled Micellar Nanocomplexes Comprising Green Tea Catechin Derivatives and Protein Drugs for Cancer Therapy. *Nat. Nanotechnol.* **2014**, *9*, 907−912.
(16) Zhang, Z. J.; Wang, L. M.; Wang, J.; Jiang, X. M.; Li, X. H.; Hu, Z. J. Y.; Ji, H.; Wu, X. C.; Chen, C. Y. Mesoporous Silica-Coated Gold Nanorods as a Light-Mediated Multifunctional Theranostic Platform for Cancer Treatment. *Adv. Mater.* **2012**, *24*, 1418−1423.
(17) He, Q.; Shi, J.; Chen, F.; Zhu, M.; Zhang, L. An Anticancer Drug Delivery System Based on Surfactant-Templated Mesoporous Silica Nanoparticles. *Biomaterials* **2010**, *31*, 3335−3346.
(18) Xie, M.; Shi, H.; Ma, K.; Shen, H.; Li, B.; Shen, S.; Wang, X.; Jin, Y. Hybrid Nanoparticles for Drug Delivery and Bioimaging: Mesoporous Silica Nanoparticles Functionalized with Carboxyl Groups and a Near-Infrared Fluorescent Dye. *J. Colloid Interface Sci.* **2013**, *395*, 306−314.
(19) Li, W.; Zhao, D. Extension of the Stöber Method To Construct Mesoporous SiO2 and TiO2 Shells for Uniform Multifunctional Core-Shell Structures. *Adv. Mater.* **2013**, *25*, 142−149.
(20) He, Q.; Shi, J. Mesoporous Silica Nanoparticle Based Nano Drug Delivery Systems: Synthesis, Controlled Drug Release and Delivery, Pharmacokinetics and Biocompatibility. *J. Mater. Chem.* **2011**, *21*, 5845−5855.
(21) Manzano, M.; Aina, V.; Arean, C. O.; Balas, F.; Cauda, V.; Colilla, M.; Delgado, M. R.; Vallet-Regí, M. Studies on MCM-41 Mesoporous Silica for Drug Delivery: Effect of Particle Morphology and Amine Functionalization. *Chem. Eng. J.* **2008**, *137*, 30−37.
(22) Rosenholm, J. M.; Linden, M. J. Development and Characterization of Novel Carrier Gel Core Liposomes Based Transmission Blocking Malaria Vaccine. *J. Controlled Release* **2008**, *128*, 157−165.
(23) Yang, Q.; Wang, S.; Fan, P.; Wang, L.; Di, Y.; Lin, K.; Xiao, F.-S. pH-Responsive Carrier System Based on Carboxylic Acid Modified Mesoporous Silica and Polyelectrolyte for Drug Delivery. *Chem. Mater.* **2005**, *17*, 5999−6003.
(24) Ding, J.; Kong, X.; Yao, J.; Wang, J.; Cheng, X. G.; Tang, B.; He, Z. W. Core-shell Mesoporous Silica Nanoparticles Improve HeLa cell Growth and Proliferation Inhibition by (-)-Epigallocatechin-3-gallate by Prolonging the Half-life. *J. Mater. Chem.* **2012**, *22*, 19926−19931.
(25) Schipper, M.; Nakayama-Ratchford, N.; Davis, C.; Kam, N.; Chu, P.; Liu, Z.; Sun, X.; Dai, H.; Gambhir, S. A Pilot Toxicology Study of Single-Walled Carbon Nanotubes in a Small Sample of Mice. *Nat. Nanotechnol.* **2008**, *3*, 216−221.
(26) Park, J. H.; Gu, L.; Maltzahn, G.; Ruoslahti, E.; Bhatia, S. N.; Sailor, M. J. Biodegradable Luminescent Porous Silicon Nanoparticles for *In Vivo* Applications. *Nat. Mater.* **2009**, *8*, 331−336.
(27) Li, L. L.; Tang, F. Q.; Liu, H. Y.; Liu, T. L.; Hao, N. J.; Chen, D.; Teng, X.; He, J. Q. *In Vivo* Delivery of Silica Nanorattle Encapsulated Docetaxel for Liver Cancer Therapy with Low Toxicity and High Efficacy. *ACS Nano* **2010**, *4*, 6874−6882.
(28) Puddu, V.; Perry, C. C. Peptide Adsorption on Silica Nanoparticles: Evidence of Hydrophobic Interactions. *ACS Nano* **2012**, *6*, 6356−6363.
(29) Townson, J. L.; Lin, Y.-S.; Agola, J. O.; Carnes, E. C.; Leong, H. S.; Lewis, J. D.; Haynes, C. L.; Brinker, C. J. Re-examining the Size/Charge Paradigm: Differing *in Vivo* Characteristics of Size- and Charge-Matched Mesoporous Silica Nanoparticles. *J. Am. Chem. Soc.* **2013**, *135*, 16030−16033.
(30) Zhang, L.; Giraudo, E.; Hoffman, J. A.; Hanahan, D.; Ruoslahti, E. Lymphatic Zip Codes in Premalignant Lesions and Tumors. *Cancer Res.* **2006**, *66*, 5696−5706.
(31) Rakovich, T. Y.; Mahfoud, O. K.; Mohamed, B. M.; Prina-Mello, A.; Crosbie-Staunton, K.; Broeck, T. V. D.; Kimpe, L. D.; Sukhanova, A.; Baty, D.; Rakovich, A.; Maier, S. A.; Alves, F.; Nauwelaers, F.; Nabiev, I.; Chames, P.; Volkov, Y. Highly Sensitive Single Domain Antibody Quantum Dot Conjugates for Detection of HER2 Biomarker in Lung and Breast Cancer Cells. *ACS Nano* **2014**, *8*, 5682−5695.
(32) Melancon, M. P.; Zhou, M.; Zhang, R.; Xiong, C. Y.; Allen, P.; Wen, X. X.; Huang, Q.; Wallace, M.; Myers, J. N.; Stafford, R. J.; Liang, D.; Ellington, A. D.; Li, C. Selective Uptake and Imaging of Aptamer- and Antibody-Conjugated Hollow Nanospheres Targeted to Epidermal Growth Factor Receptors Overexpressed in Head and Neck Cancer. *ACS Nano* **2014**, *8*, 4530−4538.
(33) Myrberg, H.; Zhang, L. L.; Mäe, M.; Langel, Ü. Design of a Tumor-Homing Cell-Penetrating Peptide. *Bioconjugate Chem.* **2008**, *19*, 70−75.


DOI: 10.1021/acsami.5b05618
*ACS Appl. Mater. Interfaces* 2015, 7, 18145−18155

(34) Cauda, V.; Schlossbauer, A.; Kecht, J.; Zürner, A.; Bein, T. Multiple Core-Shell Functionalized Colloidal Mesoporous Silica Nanoparticles. *J. Am. Chem. Soc.* **2009**, *131*, 11361−11370.



DOI: 10.1021/acsami.5b05618
*ACS Appl. Mater. Interfaces* 2015, 7, 18145−18155